




# A Simple Way of Simulating Insolation on a Rotating Body with a Commercial Solar Simulator

Selina Terliesner<sup>1</sup> · Erika Kaufmann<sup>1</sup> · Matthias Grott<sup>2</sup> · Axel Hagermann<sup>1</sup> 

Received: 24 February 2022 / Accepted: 11 April 2022  
© The Author(s) 2022

## Abstract

The surfaces of all solid bodies in the solar system, planets, moons, comets and asteroids, experience short-term temporal variations of solar irradiation which depend on their respective spin rates. These so-called insolation cycles affect temperature variations, climate, photosynthesis in plants, etc. Hence, experimental reproduction of these cycles is important for space analogue simulations. In this short note we describe a simple, low-cost method to simulate diurnal cycles in the laboratory using a type of commercial solar simulator commonly used for experimental investigation in planetary science.

**Keywords** Insolation · Thermal simulations · Solar simulator · Thermal wave

## 1 Introduction

No body in the solar system is in a 1:1 spin–orbit coupling with the sun. The resulting diurnal insolation cycle has significant influence on, for example, climatic patterns [1], atmospheric compositions [2, 3], exobase altitudes [4], ionospheric drifts [5], animals [6], plants [7, 8] bacteria [9] or even clinical depression in humans [10, 11]. Particularly in planetary science, the diurnal insolation cycle plays an important role for a large range of processes on most bodies in the solar system: it affects thermal weathering on all solid surfaces [12], dust devils on Mars [13], variations in Europa’s Exosphere [14], haze on Ceres [15], and the Yarkovsky effect on asteroids [16]. Therefore the simulation of diurnal cycles is important in several scientific fields. One way to simulate a diurnal cycle is by using dimmable lamps and various

---

This article is part of the Special Issue on Thermophysics of Advanced Spacecraft Materials and Extraterrestrial Samples.

---

✉ Axel Hagermann  
axel.hagermann@ltu.se

<sup>1</sup> SRT, Luleå University of Technology, Space Campus, Kiruna 981 92, Sweden

<sup>2</sup> Institute for Planetary Research, DLR, Rutherfordstr. 2, Adlershof, Berlin 12489, Germany

light filters (see e.g. [17]), an approach often used for biological experiments. [7] described a device that simulates sunlight intensity variations by controlling the voltage supply of a tungsten filament lamp with an external control unit consisting of a timer, a sliding potentiometer, a synchronous motor and a cam. This (non-digital) method is quite accurate for simulating the light intensity curve in terrestrial conditions. However, although tungsten filament (i.e., incandescent) lamps are easily dimmable, their irradiation power density is comparatively low and their light spectra differ significantly from the solar spectrum. In particular, UV-components of the solar radiation as observed in space are lacking in incandescent lamps and hence this method is not suitable for the simulation of diurnal cycles on extra-terrestrial bodies. Many of these bodies have no or only tenuous atmospheres which means that the insolation reaching the surface includes the UV range of the solar spectrum.

The most common way to simulate the full solar spectrum is using xenon short arc lamps. These are, however not as easily dimmable as e.g. incandescent (tungsten filament) lamps. As the power of a xenon short arc lamp can only be controlled within a few 10%, modulation of intensity has to occur in the beam path, ideally in a gradual, continuous way. Controlling the light intensity by using a polariser/analyser pair with a rotation mechanism in front of a xenon short arc lamp can be easily implemented. However, such a setup will not only change the intensity but also the irradiation spectrum. For simulations of planetary environments, the full spectrum of solar radiation is of vital importance. In particular the shorter wavelength range is relevant for, e.g., the Solid State Greenhouse Effect [18] in transparent or translucent ices, or habitability on Mars or exoplanets [19]. Hence, experiments requiring the full spectrum of solar radiation—i.e., those related to physics and chemistry on extra-terrestrial bodies—need to rely on a different method for modulating solar irradiance. For some comet-related experiments a different approach was used to avoid losing parts of the irradiation spectrum. In this case the insolation intensity from a full spectral lamp was changed using a type of step function; [20] increased and decreased irradiance stepwise, with a plateau at maximum irradiance, irradiating at each intensity level for a specific time period to simulate the changing light intensity conditions on a comet. Although this leads to more realistic intensity conditions than constant irradiation, the disadvantage of this approach is the immediate transition from nighttime to a comparatively high level of solar intensity, with neither sunrise nor sunset-like conditions.

In the following short sections, we describe a simple method to simulate the changes in insolation intensity as they arise on the surface of a rotating body in space, as it was implemented in our laboratory.

## 2 Methods

One of the operational requirements of our original setup was a close approximation of the thermal surface conditions during sunrise and sunset. A technical requirement was ease of implementation and adaptability to a wide range of rotation rates (i.e., day lengths). Limited funding as well as time constraints meant that the method had to rely on laboratory equipment already in situ. Hence, we

relied on a commercial solar simulator whose intensity is varied based on pulse width—or pulsed-duration-modulation (see e.g. [21, 22]). We would like to point out that there is at least one commercial option available to simulate variable solar light intensity: the MOS-100 system by Japanese manufacturer Bunkoukeiki Co., Ltd. can vary light intensity from a fraction of a  $\text{mW m}^{-2}$  to two solar constants. However, the effective irradiated area of this machine is limited to  $10 \times 10 \text{ mm}$ , whereas many experiments in planetary science require beam diameters in the dm range. Moreover, the geometry of the MOS-100 system makes it impossible to irradiate cooling devices and/or vacuum chambers beyond a certain size without an additional mirror arrangement. These reasons, along with the substantial impact the purchase of such a machine has on laboratory finances, makes the use of pulse-width modulation an attractive option for simulating varying-intensity solar irradiation.

## 2.1 Equipment

The solar simulator used for the simulation of diurnal variations is a widely used piece of equipment from Solar Light Company. The solar simulator is equipped with a 1000 W xenon short arc lamp (spectral range 290 to 2500 nm) and a 220 V/50–60 Hz power supply. The LS1000-6R-H-AM0 model used is an Air Mass 0 solar simulator with a  $6^\circ$  (152.4 mm), circular horizontal beam with a light intensity of  $1400 \text{ W/m}^2$  measured in a working plane  $6'$  (914.4 mm) from the collimator lens. The solar simulator has a mechanical shutter that enables the experimenter to stop irradiation without switching off the lamp. This feature is common in solar simulators, its purpose being a limitation of the number of switching cycles in order to extend the life of the xenon-arc lamp. With the type of solar simulator used in our experiments, the intensity of the irradiation can be varied by either changing the distance between the solar simulator and the working plane (i.e., the object to be irradiated) as power density decreases with distance from the light source, or by adjusting the input power. The former cannot easily be implemented automatically as the size of any laboratory limits the distance between light source and sample. Moreover, moving the entire experimental setup in order to change distance with time poses a substantial mechanical engineering challenge. Moreover, the movement would have to be periodic to simulate a diurnal cycle—and the gradual change from no irradiation to higher levels as experienced on a rotating solar system body during sunrise/sunset would still be a problem. Changing intensity by adjusting input power is limited by the properties of the power supply. For most commercially available solar simulators (except for the MOS-100 system mentioned above), the intensity can be varied between 70 and 100% of full power, although the exact irradiance output corresponding to each power setting has to be determined individually, e.g. by a pyranometer in the working plane. Either way, changing only the above settings will not result in a simulated diurnal cycle since there is always a minimum, rather high, level of intensity, as in the method used by [20]. Hence, sunrise/sunset-like scenarios cannot be simulated.

## 2.2 Conceptual Solution

The obvious way to simulate a diurnal cycle is to irradiate a sample with a half-sine intensity curve with no irradiation at night time. As pointed out above, using a commercial solar simulator, this cannot be achieved by changing the current supply of the xenon arc lamp because minimum power output is limited to some 70%. The same applies to varying the distance between the solar simulator and the target periodically. Simulating dusk–dawn transitions requires a somewhat more careful approach.

If the focus of artificial insolation experiments is the observation of a material's response to solar heating, one can make use of the thermal skin effect. As the heat from a surface temperature excursion diffuses into the subsurface, it experiences a damping (and also a lagging) effect. For a cyclical surface temperature  $T_0(t)$  of period  $P$  the amplitude of the temperature oscillation  $T_A$  decreases as

$$T_A(z) = T_0 \exp\left(-z \left[\sqrt{\frac{\pi}{P\kappa}}\right]\right), \quad (1)$$

where  $\kappa$  is the thermal diffusivity of the material. Short insolation periods  $P$  and/or low thermal conductivities  $\kappa$  thus effectively result in a low-pass filter for thermal signals as they propagate into the material from the surface. As the temperature at depth will not be affected by short-term variations in solar intensity, a diurnal cycle can be simulated by pulsing insolation intermittently using a mechanical chopper—which is easy enough to implement since commercial solar simulators tend to come equipped with a shutter. A diurnal insolation cycle is subdivided into short time increments of length  $\Delta t$  and the effective power can thus be regulated by adjusting the time  $\delta t$  during which the shutter is open over each interval  $\Delta t$ . This approach is effectively an implementation of pulse-width-modulation (PWM) (also known as pulsed-duration-modulation) which is commonly used for generating an analogue signal using a digital source. PWM is applied widely, from power conversion to communications and in PWM the average power delivered by a signal is reduced or increased by clocking it into separated parts. For the application in question, PWM resembles a switch used to turn a heater on and off. The longer the heater is on compared to the period it is turned off, the higher the time-averaged heating output. The temperature of the heated object follows the heat-on/heat-off cycle but changes more slowly due to the thermal inertia of the object.

To simulate a diurnal cycle of period  $P$ , the irradiation can be controlled by adjusting the solar simulator shutter opening time  $0 \leq \delta t \leq \Delta t$  over each  $\Delta t$  as follows:

$$\frac{\delta t}{\Delta t} = \begin{cases} \sin(2\pi t/P) & ; (N-1)P < t < (N-\frac{1}{2})P \\ 0 & ; (N-\frac{1}{2})P \leq t \leq NP \end{cases} \quad (2)$$

$$N = 1, 2, 3, \dots$$

So the proportion of the time interval over which the shutter is open,  $\delta t/\Delta t$  is modulated as a sine wave during the simulated day whilst the shutter is kept closed during the simulated night.

### 2.3 Technical Implementation

Obviously, one should choose a  $\Delta t \ll P$  as short as possible for accurate results. However, in a bid to avoid complicated mechanical chopper arrangements, one can make use of the external shutter trigger of a commercial solar simulator. The shutter of the LS1000 series solar simulators for example can be operated remotely via a DE-9 connector. In order to limit the number of switching cycles (and thus wear of the shutter mechanism), we considered a  $\Delta t$  between 30 s and several minutes to be practical. This figure is also reasonable because most solar system bodies have rotation rates exceeding a few hours. We estimate the shutter opening/closing time to be below 0.1 s range, hence we would not recommend our setup to be used for objects with rotation periods faster than 20–30 min, because the accuracy of  $\delta t/\Delta t$ , and hence the resulting intensity sine wave will be affected.

Regarding any temperature measurements in the irradiated material, one should also bear in mind that depths up to the order of

$$z \approx \sqrt{\frac{\Delta t \kappa}{\pi}} \quad (3)$$

will be affected by thermal high-frequency noise of the on/off switching of the irradiation. We used a programmable power supply (Rhode & Schwarz HMC8042) connected to a relay which triggers the internal shutter of the LS1000 simulator. The power supply can be fed with a csv table of  $\delta t$  values via a USB memory stick. Once at the end of the programmed table, the switching cycle is repeated. It should be noted that, apart from mechanical wear, another lower limit on the  $\Delta t$  is imposed by the available memory of the power supply. Hence, the choice of  $\Delta t$  involves a careful consideration of trade-offs between insolation period and cycle length, size and type of sample material, power supply memory and total wear permissible. For those reasons, we ended up with values between 30 and 60 s. A schematic sketch of the setup is shown in Fig. 1.

## 3 Test Cases

We present two test cases that were used to verify our approach. For our first test case, we aimed to create idealised conditions by using a compact sample material into which thermal sensors could be embedded easily with good thermal contact.

### 3.1 Modelling Clay

In the first test case we irradiated a cylindrical (or, to be more accurate, a slightly conical) sample container with a diameter of 100 mm and a depth of 50 mm with white modelling clay with a light signal representing a diurnal cycle of 6 h length. Modelling clay was used because it is a compact material, can be moulded easily, so that exact positioning of thermal sensors inside the sample can be achieved,

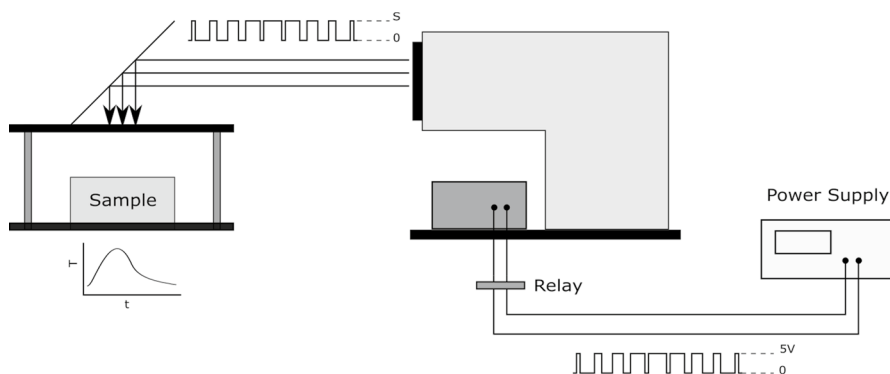


**Fig. 1** Setup of our method highlighting the simplicity of the approach. The relay switching the solar simulator shutter is operated by a 5 V pulse of varying duration. Opening and closing the shutter leads to a light pulse of full intensity  $S$ . Although the absolute irradiation intensity at the sample surface is the same for each time slot during which the shutter is open, the varying pulse length results in a temperature distribution inside the sample as would be observed in case of a constant irradiation with varying intensity, as explained in the text.

with good thermal contact. The thermal properties of modelling clay (specifically, Van Aken Plasticine) have been measured by [23], giving a thermal diffusivity  $\kappa \approx 0.3 \text{ mm}^2 \text{ s}^{-1}$  of the sample material. The constraints of our specific power supply model resulted in a choice of  $\Delta t = 43.72 \text{ s}$ . This specific value was chosen because it allows for the highest achievable accuracy within the limits given by the power supply whose internal memory was limited to 0.5 kB. Bearing in mind Eq. 3, depths up to some mm can be expected not to be significantly affected by temperature excursions caused by the light switching cycle.

We present the results of this test case in Fig. 2. Pt-100 temperature sensors were embedded at depths 1 mm, 10 mm and 20 mm. The sample is not exposed to insolation at the start of the experiments, hence a new thermal equilibrium needs to be established. This is visible as a gradual increase of the minimum temperature. As expected, the near-surface sensor at a depth of 1 mm is affected by the modulation of the light intensity, although the amplitude of this high-frequency noise is less than 0.2 K at 1 mm depth, which is negligible compared to a peak-to-peak amplitude of 14 K. For opaque materials such as modelling clay it might not be necessary to use a full spectrum solar simulator for all types of investigations, although it is generally recommended to do so for experiments of materials under extraterrestrial conditions. Modelling clay was only chosen as a proxy for the practical reasons pointed out above; after all, the purpose of this study is a proof of concept of pulse width modulation for space experiments.

### 3.2 Artificial Snow

Simulated diurnal insolation cycles are often used to investigate the behaviour of ices on solar system bodies, for example in relation to the Martian polar regions [24] or comets [20]. Here, the accurate reproduction of the temperature evolution at

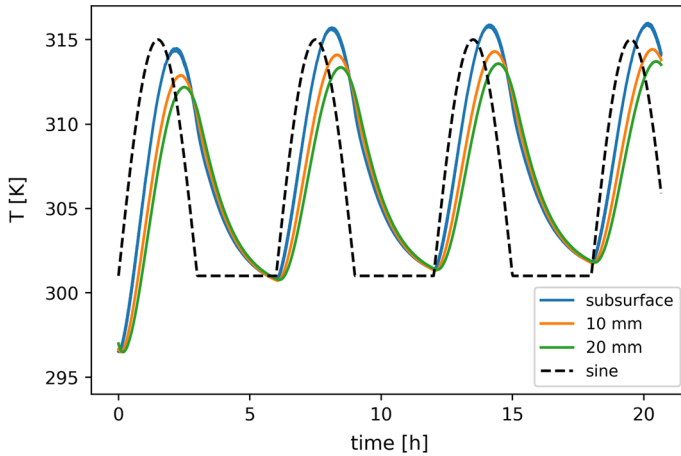


**Fig. 2** Temperature as measured within a modelling clay sample exposed to full-spectrum solar radiation pulse-width-modulated to simulate a diurnal wave of 6 h duration. Temperatures were measured at a depth of 1 mm (blue), 10 mm (orange), and 20 mm (green). The normalised light intensity is overlaid as a black dashed line (Color figure online).

depth is important for understanding phenomena such as outgassing or sintering. In a non-translucent material, heat is conducted purely by conduction, hence one can expect the temperatures at depth not to be affected by the pulse width modulation. However, as ices are translucent for a large part of the solar spectrum, thermal sensors at depth might be affected directly by the pulsing of the simulated insolation when used in ices.

In order to assess the suitability of the method for translucent media, we used a sample of artificial snow, i.e., granular water ice with a pore volume of approximately 55% (see e.g. [25] for a detailed description of the material's properties and production). Note that granular water ice formed the base of many a sample in the KOSI comet simulation experiments in the 1990s (see e.g. [20]). Hence, we will refer to our experiments as mock comet simulations—without expressing a judgment as to whether this material can still be considered a suitable comet analogue in the post-Rosetta era.

In this test case, the diurnal cycle length was 2 h. Here, a longer  $\Delta t = 60$  s results in a larger depth affected by short-period thermal noise from the pulsing. We ran a mock comet simulation as a worst case, i.e. used similar conditions to [25] in that the sample was 124 mm in diameter, 150 mm high and in vacuum, on a base plate kept at a temperature of 173 K. Pt-100 sensors were embedded at depths 1, 20, 30 and 50 mm below the surface. This simulation was meant to maximise light penetration of the sample and minimize light absorption at the surface, hence granular, pure ice was used. Figure 3 shows no indications of the thermal sensors at depth within the samples being affected by the pulsing. Recalling Eq. 3, we note that, although  $\Delta t$  is higher than in the previous test case, the larger depth of the topmost sensor combined with the *lower* thermal diffusivity of artificial snow results in an effective damping of the thermal pulse.

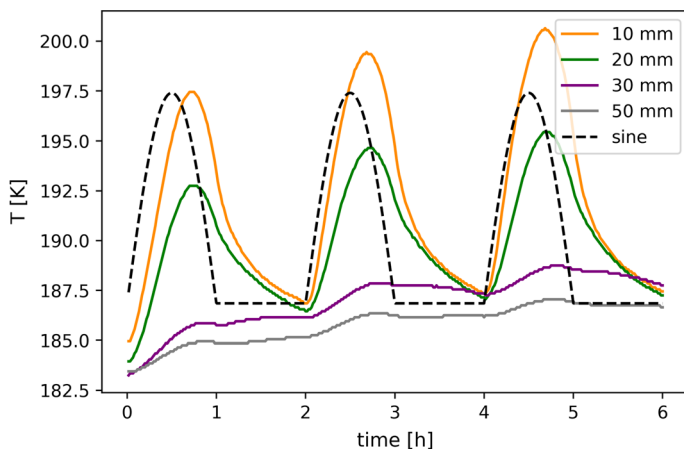


**Fig. 3** Temperature as measured during a mock comet simulation experiment with a diurnal period of 2 h. Temperatures were measured at 10 mm below the surface (orange), 20 mm below the surface (green), 30 mm below the surface (purple) and 50 mm below the surface (grey). The normalised light intensity is overlaid in a black dashed line. The experiment was carried out in vacuum. Note that the sample was not in thermal equilibrium with the time-averaged radiation balance at the start of the experiment, resulting in an increase in temperature cycle maxima and minima (Color figure online).

Light absorption by the Pt-100 evidently does not play a prominent role, either. Hence we can recommend our simple setup for experiments related to icy surfaces.

## 4 Conclusion

We have presented a simple and effective way of simulating diurnal insolation cycles, as they occur on solar system bodies, in the laboratory. The method relies on applying pulse-width-modulation, administered to the shutter of a commercial solar simulator by means of a programmable power supply. As no bespoke parts of specialised equipment are needed, the costs of implementing this solution are negligible. In our case, only a relay costing less than EUR 5 was required.

Using shutter opening times of a few seconds, any thermal noise caused by the pulsing of the radiation is dissipated within a depth of a few mm, even in a medium like modelling clay, whose thermal diffusivity is high compared to the regolith found on many planetary surfaces.

This simple method cannot accurately reproduce all of the phenomena related to sunrise or sunset, such as varying shadow length, or the effect of surface roughness. However, the method enables investigation of the effects of a gradual power density increase or decrease over the course of a day.

**Funding** Open access funding provided by Lulea University of Technology.



**Open Access** This article is licensed under a Creative Commons Attribution 4.0 International License, which permits use, sharing, adaptation, distribution and reproduction in any medium or format, as long as you give appropriate credit to the original author(s) and the source, provide a link to the Creative Commons licence, and indicate if changes were made. The images or other third party material in this article are included in the article's Creative Commons licence, unless indicated otherwise in a credit line to the material. If material is not included in the article's Creative Commons licence and your intended use is not permitted by statutory regulation or exceeds the permitted use, you will need to obtain permission directly from the copyright holder. To view a copy of this licence, visit <http://creativecommons.org/licenses/by/4.0/>.

## References

1. J. Yin, A. Porporato, Diurnal cloud cycle biases in climate models. *Nat. Commun.* **8**, 1–8 (2017). <https://doi.org/10.1038/s41467-017-02369-4>
2. H. Brinton, H. Taylor Jr., H. Niemann, H. Mayr, A. Nagy, T. Cravens, D. Strobel, Venus nighttime hydrogen bulge. *Geophys. Res. Lett.* **7**, 865–868 (1980). <https://doi.org/10.1029/GL0071011p00865>
3. J. Cui, M.-H. Fu, Z.-P. Ren, H. Gu, J.-H. Guo, X.-S. Wu, Z.-P. Wu, H.-R. Lai, Y. Wei, Nitric oxide abundance in the Martian thermosphere and its diurnal variation. *Geophys. Res. Lett.* **47**, 2020–087252 (2020). <https://doi.org/10.1029/2020GL087252>
4. M. Fu, J. Cui, X. Wu, Z. Wu, J. Li, The variations of the Martian exobase altitude. *Earth Planet. Phys.* **4**, 4–10 (2020). <https://doi.org/10.26464/epp2020010>
5. J. Chen, W. Wang, J. Lei, T. Dang, The physical mechanisms for the sunrise enhancement of equatorial ionospheric upward vertical drifts. *J. Geophys. Res.* **125**, 2020–028161 (2020). <https://doi.org/10.1029/2020JA028161>
6. E.L. Unger, C.J. Earley, J.L. Beard, Diurnal cycle influences peripheral and brain iron levels in mice. *J. Appl. Physiol.* **106**, 187–193 (2009). <https://doi.org/10.1152/jappphysiol.91076.2008>
7. C.M. Boyd, J. Marra, A device to simulate the variability in sunlight intensity for laboratory cultures of algae. *J. Fish. Res. Board Can.* **35**, 1152–1154 (1978). <https://doi.org/10.1139/f78-181>
8. K. Masuda, T. Yamada, Y. Kagawa, H. Fukuda, Time lag between light and heat diurnal cycles modulates circadian clock association 1 rhythm and growth in *Arabidopsis thaliana*. *Front. Plant Sci.* **11**, 2291 (2021). <https://doi.org/10.3389/fpls.2020.614360>
9. R. Liu, Y. Liu, Y. Chen, Y. Zhan, Q. Zeng, Cyanobacterial viruses exhibit diurnal rhythms during infection. *Proc. Natl. Acad. Sci. USA* **116**, 14077–14082 (2019). <https://doi.org/10.1073/pnas.1819689116>
10. A.P.R. Moffot, R.E. O'Carroll, J. Bennie, S. Carroll, H. Dick, K.P. Ebmeier, G.M. Goodwin, Diurnal variation of mood and neuropsychological function in major depression with melancholia. *J. Affect. Disord.* **32**, 257–269 (1994). [https://doi.org/10.1016/0165-0327\(94\)90090-6](https://doi.org/10.1016/0165-0327(94)90090-6)
11. P.R. Joyce, R.J. Porter, R.T. Mulder, S.E. Luty, J.M. McKenzie, A.L. Miller, M.A. Kennedy, Reversed diurnal variation in depression: associations with a differential antidepressant response, tryptophan: large neutral amino acid ratio and serotonin transporter polymorphisms. *Psychol Med.* **35**, 511–517 (2005). <https://doi.org/10.1017/s0033291704003861>
12. J. Molaro, S. Byrne, Rates of temperature change of airless landscapes and implications for thermal stress weathering. *J. Geophys. Res. (Planets)* **117**, 10011 (2012). <https://doi.org/10.1029/2012JE004138>
13. R.M. Chapman, S.R. Lewis, M. Balme, L.J. Steele, Diurnal variation in Martian dust devil activity. *Icarus* **292**, 154–167 (2017). <https://doi.org/10.1016/j.icarus.2017.01.003>
14. A.V. Oza, F. Leblanc, R.E. Johnson, C. Schmidt, L. Leclercq, T.A. Cassidy, J.-Y. Chaufray, Dusk over dawn O<sub>2</sub> asymmetry in Europa's near-surface atmosphere. *Planet Space Sci.* **167**, 23–32 (2019). <https://doi.org/10.1016/j.pss.2019.01.006>
15. G. Thangjam, M. Hoffmann, A. Nathues, J.-Y. Li, T. Platz, Haze at Occator crater on dwarf planet Ceres. *Astrophys. J.* **833**, 25 (2016). <https://doi.org/10.3847/2041-8213/833/2/L25>
16. O. Golubov, Y. Kravets, Y.N. Krugly, D.J. Scheeres, Physical models for the normal YORP and diurnal Yarkovsky effects. *Mon. Not. R. Astron. Soc.* **458**, 3977–3989 (2016). <https://doi.org/10.1093/mnras/stw540>

17. C. Poulin, D. Antoine, Y. Huat, Diurnal variations of the optical properties of phytoplankton in a laboratory experiment and their implication for using inherent optical properties to measure biomass. *Opt. Exp.* **26**, 711–729 (2018). <https://doi.org/10.1364/OE.26.000711>
18. E. Kaufmann, N.I. Kömle, G. Kargl, Laboratory simulation and theoretical modelling of the solid-state greenhouse effect. *Adv. Space Res.* **39**, 370–374 (2007). <https://doi.org/10.1016/j.asr.2005.05.069>
19. P.B. Rimmer, J. Xu, S.J. Thompson, E. Gillen, J.D. Sutherland, D. Queloz, The origin of RNA precursors on exoplanets. *Sci. Adv.* **4**, 3302 (2018). <https://doi.org/10.1126/sciadv.aar3302>
20. ...E. Grün, J. Gebhard, A. Bar-Nun, J. Benkhoff, H. Düren, G. Eich, R. Hische, W.F. Huebner, H.U. Keller, G. Klees, H. Kochan, G. Kölzer, H. Kroker, E. Kührt, P. Lämmerzahl, E. Lorenz, W.J. Markiewicz, D. Möhlmann, A. Oehler, J. Scholz, W.F. Seidensticker, K. Roessler, G. Schwehm, G. Steiner, K. Thiel, H. Thomas, Development of a dust mantle on the surface of an insolated ice-dust mixture—results from the kosi-9 experiment. *J. Geophys. Res.* **98**, 15091–15104 (1993). <https://doi.org/10.1029/93JE01134>
21. R. Jalnekar, K. Jog, Pulse-width-modulation techniques: a review. *IETE J. Res.* **46**(3), 175–183 (2000). <https://doi.org/10.1080/03772063.2000.11416153>
22. F. Serra-Graells, R. Adoración, J.L. Huertas, *Pulse duration modulation low-voltage. CMOS log companding analog design* (Springer, Boston, 2003), pp. 137–144
23. K. Eckerson, B. Liechty, C.D. Sorensen, Thermomechanical similarity between Van Aken plasticine and metals in hot-forming processes. *J. Strain Anal. Eng. Des.* **43**, 383–394 (2008). <https://doi.org/10.1243/03093247JSA364>
24. E. Kaufmann, A. Hagermann, Experimental investigation of insolation-driven dust ejection from Mars' CO<sub>2</sub> ice caps. *Icarus* **282**, 118–126 (2017). <https://doi.org/10.1016/j.icarus.2016.09.039>
25. E. Kaufmann, A. Hagermann, Constraining the parameter space of comet simulation experiments. *Icarus* **311**, 105–112 (2018). <https://doi.org/10.1016/j.icarus.2018.03.025>